

Long-term in vivo biomechanical properties and biocompatibility of poly(2-hydroxyethyl methacrylate-co-methyl methacrylate) nerve conduits

Jason S. Belkas^a, Catherine A. Munro^a, Molly S. Shoichet^b, Miles Johnston^a,
Rajiv Midha^{a,*}

^a Division of Neurosurgery and Neuroscience Research Program, Sunnybrook and Women's College Health Sciences Centre, University of Toronto, Toronto, Ont., Canada, M4N 3M5

^b Department of Chemical Engineering and Applied Chemistry and Department of Chemistry, Institute of Biomaterials and Biomedical Engineering, University of Toronto, Toronto, Ont., Canada, M4N 3M5

Received 15 January 2004; accepted 27 May 2004

Available online 2 July 2004

Abstract

Artificial grafts are promising alternatives to nerve grafts for peripheral nerve repair because they obviate the complications and disadvantages associated with autografting such as donor site morbidity and limited tissue availability. We have synthesized poly(2-hydroxyethyl methacrylate-co-methyl methacrylate) (PHEMA-MMA) porous tubes and studied their efficacy in vivo. Specifically, we studied the short- and long-term stability and biocompatibility of 12 mm long tubes for the repair of surgically created 10 mm nerve gaps in rat sciatic nerves.

Prior to implantation, tubes were analyzed in vitro using a micro-mechanical tester to measure displacement achieved with load applied. These results served as a calibration curve, $y = 6.8105 \times -0.0073$ ($R^2 = 0.9750, n = 28$), for in vivo morphometric tube compression measurements.

In vivo, most of the PHEMA-MMA conduits maintained their structural integrity up to 8 weeks, but 29% (4/14) of them collapsed by 16 weeks. Interestingly, the tube wall area of collapsed 16-week tubes was significantly lower than those of patent tubes.

Tubes were largely biocompatible; however, a small subset of 16-week tubes displayed signs of chronic inflammation characterized by “finger-like” tissue extensions invading the inner tube aspect, inflammatory cells (some of which were ED1 + macrophages) and giant cells. Tubes also demonstrated signs of calcification, which increased from 8 to 16 weeks. To overcome these issues, future nerve conduits will be re-designed to be more robust and biocompatible.

© 2004 Elsevier Ltd. All rights reserved.

Keywords: Nerve repair; Nerve guidance channel; Compression; Inflammation; Sciatic nerve; Rat

1. Introduction

Various nerve conduits have been shown to permit peripheral nerve regeneration (reviewed in [1,2]). However, they are often not able to facilitate growth over long gaps due to collapse, scar infiltration, and, as in the case of biodegradable materials, early resorption [2]. In

this study, we utilized nerve tubes made from a non-biodegradable hydrogel material, poly(2-hydroxyethyl methacrylate-co-methyl methacrylate) (PHEMA-MMA), to repair rat sciatic nerve injury gaps because PHEMA has a long history of medical use as evidenced by over 25 years in soft contact lenses [3] and recently for drug delivery [4]. Moreover, the PHEMA-MMA tubes synthesized for these studies were designed to match the modulus of soft tissue, such as nerve [5], and to have the appropriate transport properties [6] for nerve repair. These hydrogel nerve tubes were synthesized by a liquid-liquid centrifugal casting technique using a redox-initiated polymerization in excess water

*Corresponding author. Department of Clinical Neurosciences, Division of Neurosurgery, University of Calgary, Foothills Medical Centre, Room 1195, 1403–29 Street N.W., Calgary, Alta, Canada T2N 2T9. Tel.: +1-403-944-1259; fax: +1-403-270-7878.

E-mail addresses: rajmidha@ucalgary.ca, rajiv.midha@calgaryhealthregion.ca, rajiv.midha@sw.ca (R. Midha).

with a total monomer formulation of 33% and ethylene dimethacrylate crosslinker. The resulting hydrogel tubes are cross-linked macromolecular networks of hydrophilic copolymers swollen in water [3].

Hudson et al. [7] listed several important properties that guidance channels should possess: easily fabricated with the desired dimensions and topography, implanted with relative ease, and sterilizable. PHEMA-MMA possesses these properties [5]. Additionally, conduits should be pliable enough to glide and bend with the animal's limb movements, yet stiff enough not to collapse in vivo. The ideal polymer should also be non-immunogenic, causing neither local tissue irritation nor allergic response [2]. While calcification can decrease the functional longevity of implanted devices [8] and has been observed for PHEMA-MMA [9], we chose to use PHEMA-MMA tubes because previous 8 week in vivo studies demonstrated that PHEMA-MMA tubes were biostable, incited minimal tissue reactivity, and supported nerve regeneration through their lumen [5]. The objectives of this project were to investigate the compressive moduli of these tubes in vitro and assess the stability and biocompatibility of PHEMA-MMA tubes in situ at nerve injury implantation sites over the short- and longer-term (up to 16 weeks). Specifically, several tube dimensional parameters were measured pre- and post-implantation and a detailed histological evaluation was conducted, including assessment of macrophage infiltration and micro-calcification.

2. Materials and methods

2.1. Tube preparation

All chemicals were purchased from Aldrich Chemical Co. (Milwaukee, WI, USA) and used as received unless otherwise stated. Hydrogel nerve tubes were manufactured using a technique developed by Dalton and Shoichet [10]. The PHEMA-MMA tubes utilized in this study were composed of 33% monomer of which 86% was HEMA and 14% was MMA by mass.

Briefly, the monomer mixture was injected into a silane-treated (Sigmacote, Sigma) glass cylindrical mold, with an inner diameter of 1.8 mm, which was spun horizontally along its longitudinal axis at 2500 r.p.m. at room temperature overnight. The resulting tube was composed of a gel-like outer layer that was formed by the coalescence of predominantly liquid-like phase-separated particles [10] and an inner spongy (IS) macroporous layer which likely comprised predominantly PHEMA particles.

The hydrogel nerve tubes had an inner diameter of 1.3 mm, outer diameter (OD) of 1.8 mm, and length of 12 mm. Tube cross-sections of 100- μ m thickness were taken from each end of the 12 mm long tubes and viewed

under the stereomicroscope (Leica MZ-6, Leica Microsystems, Wetzlar, Germany) in order to verify tube concentricity. The tubes were Soxhlet extracted in water overnight then sterilized by autoclaving in phosphate-buffered saline (PBS) as previously described [10] prior to both in vitro and in vivo testing.

2.2. In vitro micro-mechanical analysis

A micro-mechanical tester (Dynatek Dalta, Galena, MO, USA) was used to measure the compressive moduli of the tubes. The displacement was measured for PHEMA-MMA tubes with applied loads of: 0.5 g ($n = 6$), 1 g ($n = 5$), 2 g ($n = 4$), 3 g ($n = 4$), 4 g ($n = 4$), and 5 g ($n = 5$). The displacements of hydrated tubes were measured in room temperature distilled water and the equilibrium displacement measured for a given load. The measured displacement was the difference between the OD of the tube in the non-compressed state (displacement of 0.00 mm) and that of the tube in the compressed (at equilibrium) state. Each tube was compressed once and then discarded after recording the equilibrium displacement. These results served as a calibration curve for tube compression, in vivo.

2.3. In vivo implantation

Sterile PHEMA-MMA tubes were filled with an inner matrix formed from 1.28 mg/ml type I collagen as described recently [5]. Inbred adult male Lewis rats (250–275 g) were obtained from Harlan–Sprague–Dawley (Indianapolis, IN). All surgical procedures were performed with the aid of an operating microscope (Leica M651, Leica Microsystems, Wetzlar, Germany) in an aseptic manner according to standard microsurgical techniques, as previously described [11]. Following gluteal and posterior thigh incisions, the sciatic nerve was exposed deep to the biceps femoris muscle and an 8 mm segment of the nerve was excised which, after retraction of the nerve ends, resulted in a 10 mm nerve gap. Then a 12 mm long PHEMA-MMA tube was sutured into the resulting gap using two 10-0 nylon sutures on each side approximately 180° apart (Derma-lon, Davis and Geck, American Cyanamid Company, Danbury, CT, USA). Muscle and skin incisions were then approximated with interrupted 3-0 Polysorb (Autosuture, Norwalk, CT, USA) and continuous 3-0 silk (Autosuture, Norwalk, CT) sutures, respectively. Each rat underwent bilateral surgery.

2.4. Morphometric analysis of in vivo tube biostability

To assess tube stability and integrity, several tube parameters were compared pre- and post-implantation, morphometrically. Tube repairs were left in situ for 0 (control, $n = 5$), 4 ($n = 3$), 6 ($n = 3$), 8 ($n = 6$), and 16

($n = 4$) weeks. Following this period, animals were sacrificed by intracardiac perfusion with saline followed by 4% ice cold paraformaldehyde. The mid-portions of the tubes (approximately 4 mm long) were removed, cryopreserved in 30% sucrose for 24 h, and frozen in a Cryomatrix compound (Shandon, Pittsburgh, PA, USA). Using a cryostat, 15 μm thick cross-sections were cut, coverslipped with Permount (Fisher Scientific, Fair Lawn, New Jersey, USA) without any staining, and subsequently underwent morphometric assessment. Sections were viewed (from $40\times$ to $1000\times$) under the Olympus BX51 light microscope (Olympus America Inc., Mellville, New York, USA) with the Cool Snap-Pro camera (Media Cybernetics Inc., Silver Springs, MD, USA). Morphometric parameters measured by Image-Pro Plus (Version 4.5 for Windows) image analysis software (Media Cybernetics Inc., Silver Springs, MD, USA) included: (1) minimum (shortest) outer tube diameter, (2) the area of the tube wall, and (3) the area of the tube lumen.

2.5. General histological evaluation

Approximately 4 mm long tissue samples from the mid-portions of the tubes were harvested, fixed with glutaraldehyde, embedded in plastic, and sectioned on an ultramicrotome (Sorvall MT6000, Ivan Sorvall Inc., Norwalk, CT). These 1 μm thick cross-sections were stained with Toluidine blue and viewed under the light microscope. One cross-section from the center of each sample was taken into consideration for a general histological assessment with the aid of a light microscope. This was done for 8 ($n = 6$) and 16 ($n = 14$) week samples in an attempt to understand what cellular events may be occurring within and around the tubes *in vivo*. The software program Image Pro-Plus was used to verify the dimensions of various histological findings such as cells, nuclei, and capsules.

2.6. Qualitative macrophage analysis

The graft and its contained regenerating tissue (RT) were analyzed in the proximal and distal segments using immunohistochemical methods at 4 ($n = 3$), 8 ($n = 8$), and 16 weeks ($n = 11$) weeks post-implantation for ED1 reactivity, a marker for macrophages [12,13].

For these experiments, rats were anesthetized, perfused through the heart, and samples were collected and processed. Slides were dewaxed in three changes of xylol, dehydrated in two changes of 100% ethanol, then rinsed with a solution of PBS, 0.03% hydrogen peroxide, and 1% sodium azide. Slides were treated with 0.2% pepsin solution in Tris-Buffered Saline (TBS) at 37°C for 15 min to expose antigens and later rinsed in tap water. All incubations were done at room tempera-

ture in a humid chamber. Slides were rinsed in PBS and blocked with 7% normal horse serum for 15 min.

The primary antibody, monoclonal mouse anti-rat ED1 (MAB 1435, Chemicon International Inc., Temecula, CA, USA), was used on longitudinal sections at a dilution of 1/250 and was incubated at room temperature for 1.5 h. Sections were washed three times in TBS and then the secondary antibody (horse anti-mouse biotinylated IgG, BA 2001) was applied and incubated for 45 min. Sections were washed three times with TBS, incubated for 40 min in a commercial Vectastain ABC Kit (PK 4000, Vector Laboratories, Burlington, Ontario, Canada), washed three times with TBS, and chromagen solution (SK 4800, Vector Laboratories) was applied for 10 min. Slides were washed for 5 min in running tap water, lightly counterstained in Mayers hematoxylin (as described in [14]), and then dried overnight and coverslipped using Permount (Fisher Scientific).

2.7. Calcification analysis

In select cases at 8 ($n = 6$) and 16 ($n = 10$) weeks, the proximal and distal sections of the tube, along with the adjacent tissue and contained RT, were fixed by immersion in 10% buffered formalin, paraffin embedded, and then longitudinal sections were cut. These 8 μm sections were stained using the von Kossa method [15] to histologically examine for calcification and to quantitatively compare the calcification area percentage between 8 and 16 week tubes. The percent calcification area was calculated morphometrically at 40X according to Eq. (1):

$$\text{Calcification area\%} = \frac{\text{cross-sectional calcification tube area}}{\text{cross-sectional tube area}} \times 100\%. \quad (1)$$

These sections were placed onto Superfrost slides and immersed in 5% silver nitrate solution (Fisher Scientific). The slides were exposed to ultraviolet light for 10–20 min. Untreated silver was removed with the addition of 5% sodium thiosulfate for 2 min and rinsed in distilled water. Samples were dehydrated, cleared in xylene, paraffin embedded, and viewed under the light microscope.

3. Results

3.1. Stability of the tubes/morphometry

With the application of loads, the PHEMA-MMA tubes followed a linear pattern of displacement with an R^2 value of 0.975 for the best-fit line, $y = 6.8105x - 0.0073$ (Fig. 1).

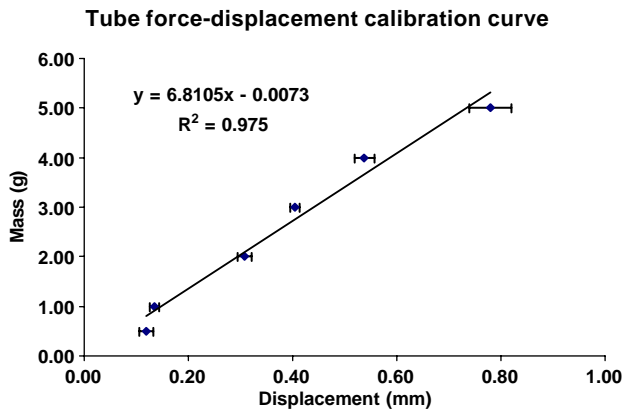


Fig. 1. The force–displacement calibration curve was linear ($R^2 = 0.975$) for the best-fit line, $y = 6.8105x - 0.0073$. Error bars denote SEM (standard error of the mean, $n = 4-6$ for each data point).

Tube OD decreased with time and this was significant ($p < 0.05$) at 8 and 16 weeks relative to $t = 0$ (Fig. 2A). The in vivo displacement was calculated by subtracting the in vivo tube ODs from that of the mean non-implanted tube OD (1.753 ± 0.017 mm). The change in tube OD (relative to pre-operated controls) increased with time and was significantly different ($p < 0.05$) by 16 weeks. These in vivo OD displacement data were compared to the in vitro calibration curve (Fig. 1) to estimate the applied load in vivo (Fig. 2B).

The area of the tube wall, including both the IS and outer gel (OG) tube layers, was measured at 0, 4, 6, 8, and 16 weeks (Fig. 2C). The areas of the tube walls were significantly lower ($p < 0.05$) at 8 and 16 weeks compared to those at $t = 0$ (Fig. 2C). This suggested that the tube wall may have thinned with time. However, none of the in vivo luminal tube areas at 4, 6, 8, and 16 weeks was significantly different than that at $t = 0$ (Fig. 2D).

3.2. Gross appearance of tubes at explantation

At all explantation time points, there was minimal adherent tissue to the tubes and tube dissection from the intermuscular plane of the sciatic nerve compartment was relatively easy. There was no evidence of gross inflammation or infection in the areas surrounding the tube. At 16 weeks, a thin glossy delicate film enveloped the tubes which also appeared to be stiffer.

Most of the tubes had an oval to round shape on sectioning at surgery. Some tubes displayed signs of collapse in that some were concave on a single side or biconcave. By visual inspection post-surgery, the dimensional properties of patent tubes were uniform along their lengths. Collapsed tubes were equally deformed at the proximal, mid, and distal levels.

3.3. Eight week PHEMA-MMA tubes

As evidenced in Fig. 3A, the tube was comprised of two layers: an IS and an OG. The RT tapered relatively little from the inner aspect of the tube (Fig. 3A). There was relatively little reactivity along the outer aspect of the 8-week tubes. The IS layer at 8 weeks was usually devoid of inflammatory cells and remained relatively intact. There were several discrete regions in the IS layer that were invaded by finger-like tissue extensions emanating from the periphery of the RT (Fig. 3A). The cells within these projections (based on morphology) included myelinated axons, fibroblasts, Schwann cells, and inflammatory cells (monocytes, lymphocytes, and macrophages). One of the six (17%) 8 week tubes had a 90% or more reduction in tube OD compared to the $t = 0$ mean tube OD.

3.4. Sixteen-week PHEMA-MMA tubes

Vascularized regenerative tissue was seen in 10/14 (71%) mid-portions of the tubes at 16 weeks (Fig. 3B). Within the RT, the myelinated axons observed were of a size, shape, number, and myelin area to indicate that the polymeric tube permitted axonal regeneration [16]. The RT was also reasonably abundant with unmyelinated nerve fibres and blood vessels. As compared to 8 weeks, the 16-week tubes at mid-level were invaded by many more finger-like projections originating from the RT. No cells were found within the gel-like layer of the tube wall. Four of the 14 samples (29%) at 16 weeks had no RTs and 75% (3/4) of these tubes collapsed by at least 90% of their original tube OD.

This 16 week bimodal tube response is comprehensively reported elsewhere [17], in which the minority of tubes that collapsed demonstrated lower values in 10 histomorphometric and four electrophysiological parameters, as well as a lower end-target mean muscle mass.

3.5. Chronic inflammation at 16 weeks

The 16-week tube samples were examined histologically to better investigate whether cellular events had led to a higher incidence of tube collapse at 16 versus 8 weeks post-implantation. A vascularized fibrous capsule (FC), densely packed with flattened cells such as fibroblasts, formed around all of the tubes ($n = 14$) which could be seen both grossly during surgery and microscopically in the tissue sections (Figs. 3B–D). The thickness of this capsule ranged from 65 to 100 μm in the 16 week, Toluidine blue-stained tube samples. There were a number of cells that had the histological appearance suggestive of fibroblast-like cells breaching the exterior of the tube wall (Fig. 3D).

In addition, “finger-like” extensions of tissue from the RT were reaching into the IS layer of the tube in the 10

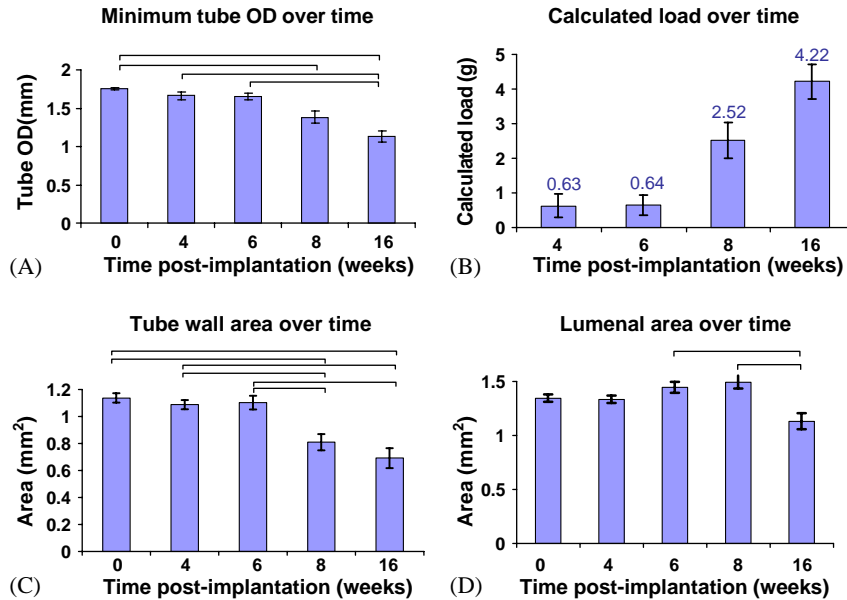


Fig. 2. (A) The minimum ODs of the tubes decreased with time in vivo and were significantly smaller ($p < 0.05$) at 8 and 16 weeks relative to $t = 0$. (B) The applied in vivo loads were estimated by comparison to the in vitro calibration curve (Fig. 1) at: 0.63 ± 0.33 , 0.64 ± 0.29 , 2.52 ± 0.52 , and 4.22 ± 0.51 g for 4, 6, 8, and 16 weeks, respectively. (C) The cross-sectional tube wall area at mid-level decreased significantly ($p < 0.05$) after 8 and 16 weeks relative to earlier time points. (D) The in vivo tube lumenal areas at 4, 6, 8, and 16 weeks were not significantly different from the pre-operated tubes at $t = 0$. The tube lumenal area at 16 weeks was significantly less ($p < 0.05$) than that at 6 and 8 weeks, but not as compared to earlier times. Connecting lines above the bars indicate significant differences obtained by ANOVAs and post hoc independent sample t -tests using the Scheffé method ($p < 0.05$). Error bars denote standard error of the mean.

samples that exhibited an RT at 16 weeks (Fig. 3E). There was also evidence of a granulomatous inflammation in which multinucleated foreign-body-type giant cells were observed at the interface between the RT and the inner tube layer (Fig. 3F). Large vacuoles were observed within these giant cells and some of these giant cells were ED1+.

3.6. ED1 macrophage and von kossa calcification examination

There were very few ED1+ macrophages in the 8 week tube samples; most of them were near the IS layer (Fig. 4A). The outer edges of the tube wall (TW) at 8 weeks and in discrete areas within the RT showed some evidence of calcification as did isolated regions of the IS layer (Fig. 4B).

At week 16, the ED1+ macrophages predominated in the center of the RT while a smaller number of reactive macrophages were located in the IS layer and external edges of the tube (Fig. 4C). No ED1+ cells were found within the gel-like layer of the tube. Most of the IS layer of the 16-week tubes exhibited considerable calcification (Fig. 4D). Furthermore, a thin film (5–10 μm) of micro-calcification was noticeable on the exterior edge of the tubes (Fig. 4D). The percent calcification of the total tube wall cross-sectional area at 16 weeks was significantly higher ($29.53 \pm 6.69\%$) than at 8 weeks ($7.44 \pm 0.44\%$) according to an independent sample t -test.

3.7. Comparison of 16-week collapsed and non-collapsed tubes

To gain greater insight as to why 29% of the 16 week tubes collapsed, a gross histological inspection of Toluidine blue-stained tubes was performed and revealed that the collapsed tubes had either little or, in most cases, no IS layer (compare Figs. 5A to B). Unlike the 16-week patent tubes, no cells invaded the inner walls of the 16 week collapsed tubes (Fig. 5B). There was no noticeable difference with inflammation on the outer tube wall between collapsed and non-collapsed tubes.

The IS layer area was significantly ($p < 0.05$) smaller in collapsed tubes ($0.1576 \pm 0.0195 \text{ mm}^2$) versus the patent tubes ($0.5578 \pm 0.0488 \text{ mm}^2$). Similarly, the entire tube wall areas (including both inner and outer layers) of collapsed tubes ($0.7506 \pm 0.0234 \text{ mm}^2$) were significantly less ($p < 0.05$) than those of non-collapsed ones ($1.3053 \pm 0.0520 \text{ mm}^2$). The OG like area in collapsed tubes ($0.5930 \pm 0.0311 \text{ mm}^2$) was lower than that in patent tubes ($0.7474 \pm 0.0438 \text{ mm}^2$) but the difference was not significant.

In vitro, the PHEMA tubes followed a linear force–displacement curve, $y = 6.8105 \times -0.0073$. Using this curve, the loads applied in vivo at 4, 6, 8, and 16 weeks (based on tube morphometry at explantation) were estimated to be 0.63 ± 0.33 , 0.64 ± 0.29 , 2.52 ± 0.52 , and 4.22 ± 0.51 g, respectively. For four of 14 or 29% of nerve conduits, the minimum tube OD progressively

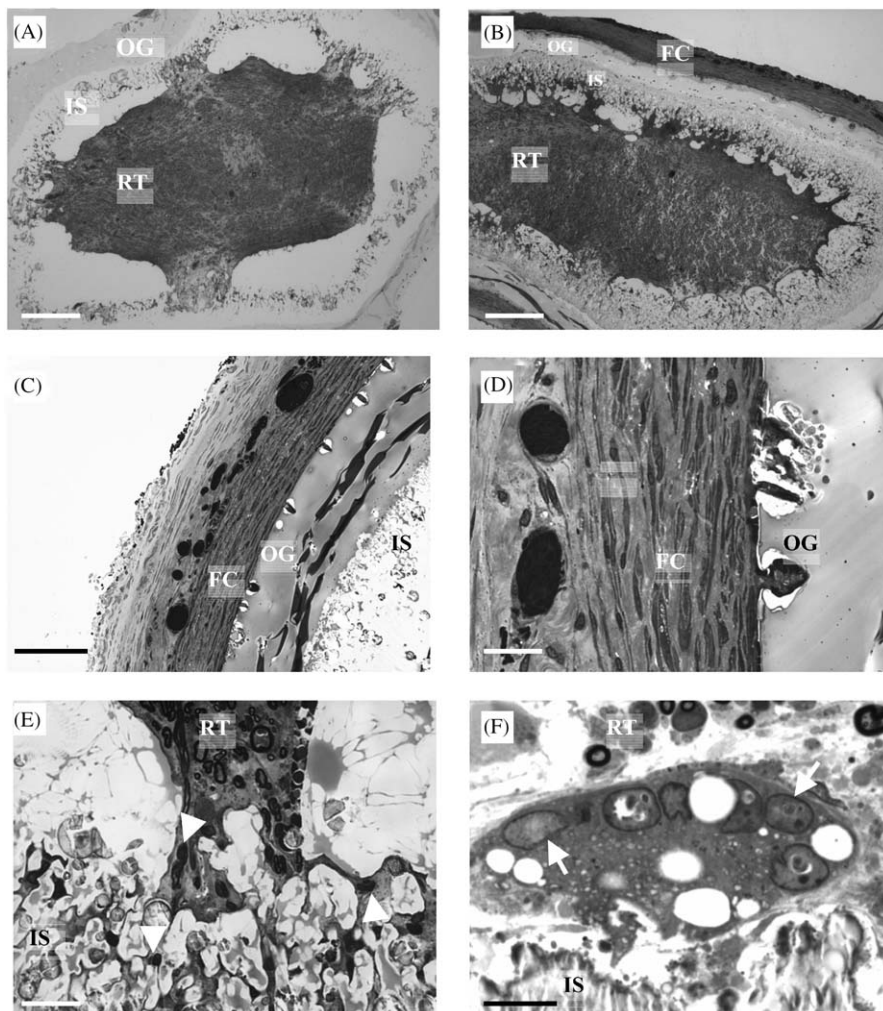


Fig. 3. (A) Low-power photomicrograph of a representative 8 week tube in cross-section, comprised of IS and OG layers, with its contained RT. (B) Low-power photomicrograph of a tube at 16 weeks with a contained RT and IS and OG layers. The tube was enveloped by a vascularized fibrous capsule (FC). (C) Photomicrograph of the dense external vascularized FC at 16 weeks, partly comprised of fibroblasts, and the cellular invagination in the OG layer. (D) Medium power photomicrograph of the outer aspect of a 16 week tube, possibly being invaginated by fibroblasts. (E) A “finger-like” tissue extension from the RT that contained some inflammatory cells (arrowheads). (F) A multi-nucleated foreign-body-type giant cell found in the IS layer of a 16 week tube, near the RT. Arrows point to some of the nuclei within these cells. Scale bars in (A) and (B) are 200 μm , (C) 100 μm , (D) and (E) 20 μm , and (F) 10 μm .

decreased over time in vivo signifying tube collapse. The tube wall area at 8 and 16 weeks was significantly lower than that of earlier time points. Interestingly, the tube wall area of collapsed 16-week tubes was significantly lower than that of their patent counterparts.

The RT within the nerve guides tapered relatively little from the inner aspect of the tubes. Eight week tubes were largely biocompatible, however, by 16 weeks, vascularized fibrous capsules enveloped the tubes from the exterior and a substantial number of “finger-like” tissue extensions containing inflammatory and giant cells invaded some of the tubes from the interior. ED1 + macrophages appeared mainly in the center of the RT. The amount of calcification of the conduits almost quadrupled from 8 to 16 weeks.

4. Discussion

The nerve conduit tubes follow a linear in vitro load–displacement curve as illustrated by the high R^2 value of 0.975 indicating the highly reproducible nature of the tube manufacturing process [10,18]. Since the gel layer is primarily responsible for the tubes’ mechanical properties [6], there may exist differences in the spongy layer that are not accounted for during the in vitro micro-mechanical testing. In the in vivo experiments, by 8 weeks post-surgery, five of six tubes remained patent and one of six (or 17%) of the tubes collapsed whereas by 16 weeks post-surgery, a bimodal population of tubes was observed in which a majority of the tubes (71%) remained patent while the other 29% collapsed.

Biological events that unfolded over time may have played key roles in causing tube collapse; however, because these were different tubes, a clean correlation is not possible, and there may have been differences in the tube inner layer morphology that resulted in different tissue regeneration/response. All systematic biases related with tube implantation that could be identified

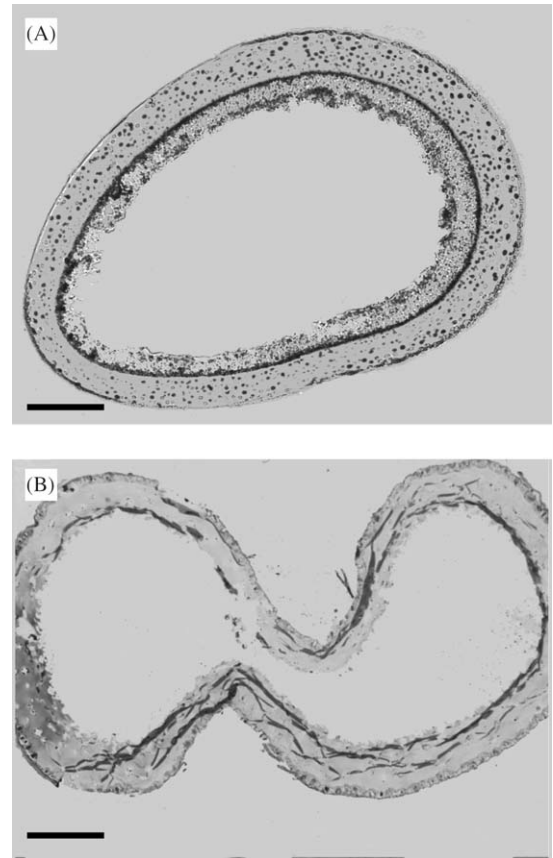
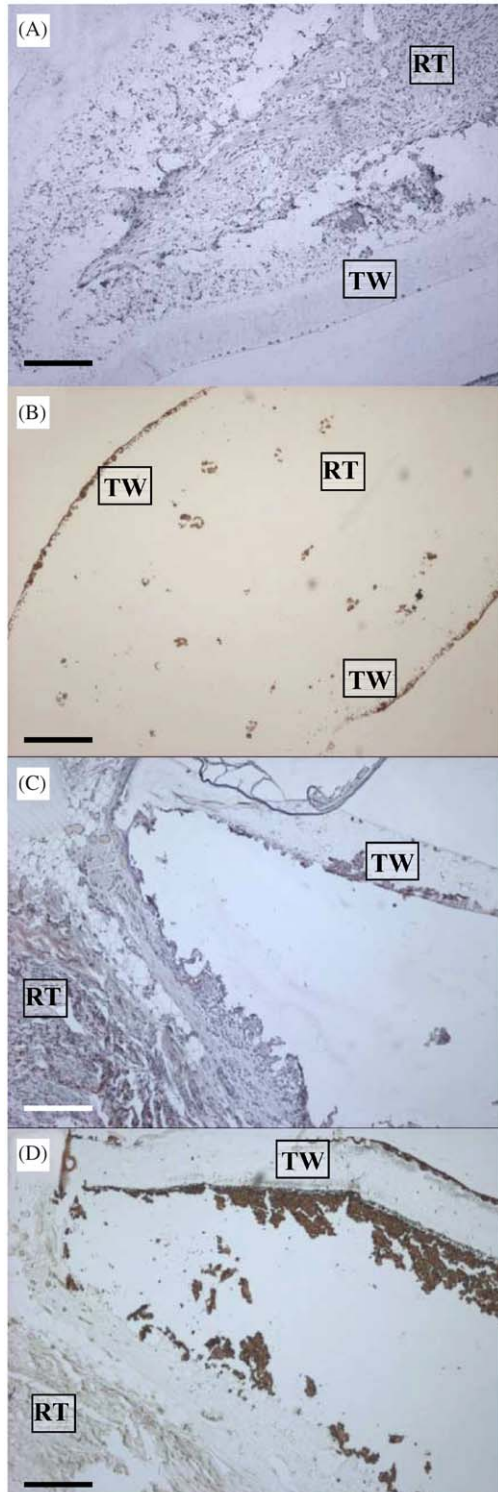


Fig. 5. Photomicrographs of mid-graft cross-sections of (A) patent tube at 16 weeks and (B) collapsed tube at 16 weeks. Scale bars are 200 μm .

were ruled out as the cause of tube collapse (such as rat side, surgical techniques, date and time of implantation, rat mass, and post-surgery collaring of certain rats).

From the *in vitro* force–displacement calibration curve and the *in vivo* morphometric tube OD measurements, compression was translated into calculated load. However, this load is really an estimate because there are several differences between the *in vitro* micro-mechanical tester and the *in vivo* environment. For example, the temperature, pH, and osmolality of the solution in which tubes were examined in the apparatus were not physiological. The tubes, *in vitro*, were not

←
 Fig. 4. (A) There were relatively few macrophages found in the 8 week tube samples immunostained with ED1, most of which were near the IS layer of the tube wall (TW) at the periphery of the RT. (B) Calcification was observed along the outer edges of the TW at 8 weeks and in discrete areas within RT and at the wall's inner layer using the von Kossa staining method. (C) At 16 weeks, ED1+ macrophages were present mostly in the center of the RT and some in the RT's periphery by the IS layer. Processing has artifactually caused the tube wall to physically separate from the rest of this sample here and in panel D. ED1 stain. (D) A serial longitudinal von Kossa-stained section of (C). The inner aspect of the 16 week tube wall was heavily calcified with modest calcification along the outer tube wall edge. Scale bars are 200 μm .

sealed whereas, *in vivo*, they were sutured to each stump. *In vitro*, a single compressive load was used to test each tube whereas *in vivo*, the loads were likely applied constantly or repetitively and potentially from multiple angles. Since the *in vivo* morphometric measurements were based on tubes that, at 8 and 16 weeks, had significantly thinner walls than the *in vitro* tubes, the calculated load values represent a maximum estimate of the actual *in vivo* load (assuming a thinner tube compresses more at a given load). Therefore, the *in vitro* test provides an approximate upper limit of how much the tubes need to be strengthened to withstand *in vitro* loads and perhaps *in vivo* loads.

Collapse of nerve tubes is not a new phenomenon and has been observed since the early tubulation experiments and shown to obstruct nerve regeneration [19–23]. The area of the tube wall is an important factor in tube biostability [24]. The area occupied by the IS layer of 16 week collapsed tubes was significantly less than that of 16 week patent tubes, which suggests that either the spongy layer was degraded over the 16 week period or the layer was missing in those tubes that collapsed. The former argument is supported by an apparent “thinning” of the tube wall as evidenced by a decrease in the mean tube wall thickness over time (Fig. 2C). The tube wall area may have decreased due to repetitive compressive forces [4], loss of material due to phagocytosis and chronic wear and tear forces [25], or simply because the regions of considerable contortion where the collapsed tubes are most deformed visibly account for less area (as in the lower tube cusp in Fig. 5B). The latter argument (that is, missing spongy layer) is supported by a lack of RT which was likely enhanced by the greater surface area of the spongy layer. Without a spongy layer, the tissue may not have been able to regenerate. Alternatively, as the sciatic nerves of the rats regenerated over time, associated with improved rat lower limb function, the nerve tubes may have experienced higher mechanical stresses possibly leading to the increased number of collapsed tubes.

Ratner et al. [4] reported that relatively smooth surfaces such as those on breast implants (and the outer surface of our tubes) were invaginated with macrophages, while rougher surfaces such as those on expanded poly(tetrafluoroethylene) (ePTFE) vascular prostheses (and the luminal surface of our tubes) elicited a foreign-body-type reaction composed of macrophages and giant cells. Likewise, high surface area-to-volume ratio implants (such as fabrics) have higher ratios of macrophages and giant cells at the implantation site than smooth surface implants which have fibrosis as a significant component at the site. This is also similar to the histological findings of the inner and outer 16-week nerve tube surfaces, respectively. Thus, there may be some phagocytosis of the IS layer that accounts for the overall reduction in tube wall area.

The vasculature within the RT may be the source of macrophages as the location of these cells was predominant in the center of this tissue rather than in the periphery (Fig. 4C). The histological findings of inflammation in this report are similar to those observed by others who have implanted PHEMA. For example, subcutaneously implanted collagen-PHEMA hydrogels in rats evoked an acute and then a chronic inflammatory response by 6 months characterized by the migration of macrophages and foreign-body giant cells while an 11 μm thick fibrous capsule formed around the implant after 1 month [26]. No necrosis, tumorigenesis, infection, or other adverse tissue reactions were observed at the implant site, indicating that the hydrogels were well-tolerated, non-toxic, and biocompatible. Others have found PHEMA orbital implants in rabbits to be well-tolerated despite the presence of fibroblasts and inflammatory cells [27]. We also found that our PHEMA tubes were biocompatible, although not totally inert given the presence of a fibrous capsule (65–100 μm) and some foreign-body-type giant cells.

The regions where most inflammatory cells were observed in the mid-tube cross-sections were the same where calcification was observed, that is, at or near the IS layer. The extent to which immunologic processes contribute to calcified tissue is poorly known [8]. Some studies on atherosclerosis have shown an association of inflammation and calcification, but the causal connection is very complex [28,29] and still controversial. Several studies have reported inflammatory cells in areas of ectopic bone protein expression [30,31]. It is widely accepted that mechanical stress stimulates calcification [8,32,33]. This may explain why there is more calcification in 16-versus 8-week tubes as the tubes may slide and bend chronically within the intermuscular pocket.

5. Conclusion

PHEMA-MMA tubes were manufactured in a highly reproducible manner as evidenced by the linear *in vitro* force–displacement curve. These tubes maintained their structural integrity and biocompatibility over 8 weeks with a minority of the tubes collapsing by 16 weeks possibly due to either a decreased (or missing) inner spongy layer or degradation, chronic inflammation, and calcification. In ongoing studies, we are investigating methods to improve the long-term stability and biocompatibility of nerve guidance channels.

Acknowledgements

We are grateful for the invaluable guidance and advice supplied by Drs. Paul Dalton and Isabelle Aubert and would like to thank Bev Young, Joyce Chan, and

Rita van Bendegem for assistance with tissue and histology preparation. This project was funded in part by the Ontario Neurotrauma Foundation (Grant # ONAO-99100), the Physicians' Services Incorporated Foundation (Grant # 01-28) and the Canadian Institute of Health Research (Grant # MOP53221). Fellowship and salary support for J.B. provided by PREA (Premier's Research Excellence Award), the 2001 and 2002 Institute of Medical Science (University of Toronto) Graduate Student Fellowships, and the 2001–2002 and 2002–2003 James F. Crothers Family Fellowships in Peripheral Nerve Damage.

References

- [1] Dahlin LB, Lundborg G. Use of tubes in peripheral nerve repair. *Neurosurg Clin N Am* 2001;12(2):341–52.
- [2] Doolabh VB, Hertl MC, Mackinnon SE. The role of conduits in nerve repair: a review. *Rev. Neurosci.* 1996;7:47–84.
- [3] Peppas NA. *Hydrogels in medicine and pharmacy*. Boca Raton, FL: CRC Press; 1987.
- [4] Ratner BD, Hoffman AS, Shoen FJ, Lemons JE. *Biomaterials science: an introduction to materials in medicine*. London: Academic Press; 1996.
- [5] Midha R, Munro CA, Dalton PD, Tator CH, Shoichet MS. Growth factor enhancement of peripheral nerve regeneration through a novel synthetic hydrogel tube. *J Neurosurg* 2003;99(3):555–65.
- [6] Luo Y, Dalton PD, Shoichet MS. Investigating the properties of novel poly(2-hydroxyethyl methacrylate-co-methyl methacrylate) hydrogel hollow fiber membranes. *Chem. Mater.* 2001;13:4087–93.
- [7] Hudson TW, Evans GR, Schmidt CE. Engineering strategies for peripheral nerve repair. *Clin Plast Surg* 1999;26(4):617–28, ix.
- [8] Schoen FJ, Levy RJ. Founder's Award, 25th Annual Meeting of the Society for Biomaterials, perspectives. Providence, RI, April 28–May 2, 1999. Tissue heart valves: current challenges and future research perspectives. *J Biomed Mater Res* 1999;47(4):439–65.
- [9] Imai Y, Masuhara E. Long-term in vivo studies of poly(2-hydroxyethyl methacrylate). *J Biomed Mater Res* 1982;16(5):609–17.
- [10] Dalton PD, Shoichet MS. Creating porous tubes by centrifugal forces for soft tissue application. *Biomaterials* 2001;22(19):2661–9.
- [11] Midha R, Munro CA, Mackinnon SE, Ang LC. Motor and sensory specificity of host nerve axons influence nerve allograft rejection. *J Neuropathol Exp Neurol* 1997;56(4):421–34.
- [12] Dijkstra CD, Dopp EA, Joling P, Kraal G. The heterogeneity of mononuclear phagocytes in lymphoid organs: distinct macrophage subpopulations in the rat recognized by monoclonal antibodies ED1, ED2 and ED3. *Immunology* 1985;54(3):589–99.
- [13] Damoiseaux JG, Dopp EA, Calame W, Chao D, MacPherson GG, Dijkstra CD. Rat macrophage lysosomal membrane antigen recognized by monoclonal antibody ED1. *Immunology* 1994;83(1):140–7.
- [14] Kiernan JA. *Histological and histochemical methods: theory and practice*. Boston: Butterworth Heinemann; 2000.
- [15] Sheehan D, Hrapchak B. *The theory and practice of histotechnology*. St. Louis: Mosby; 1980.
- [16] Belkas JS, Munro C, Dalton PD, Enescu C, Goraltchouk A, Shoichet MS, et al. In vivo and in vitro evaluation of a synthetic hydrogel tube to repair rat sciatic nerve injury gaps. *J Peripheral Nerv Sys* 2003;8(Suppl. 1):5–6.
- [17] Belkas J, Munro C, Shoichet M, Midha R. Peripheral nerve regeneration through a synthetic hydrogel. *J. Restor. Neurol. Neurosci.* 2004, In Submission.
- [18] Dalton PD, Flynn L, Shoichet MS. Manufacture of poly(2-hydroxyethyl methacrylate-co-methyl methacrylate) hydrogel tubes for use as nerve guidance channels. *Biomaterials* 2002;23(18):3843–51.
- [19] Erlacher P. Experimentelle untersuchungen uber plastik und transplantation von nerv und muskel. *Arch Klin Chir* 1914;106:389–407.
- [20] Dogliotti AM. Etudes experimentales et premiere application clinique d'une nouvelle operation destine a augmenter et a equilibrer la fonction neuro-musculaire dans la paralysie partielle des nerf. *J Chir Paris* 1935;45:30–48.
- [21] Burt AS. Growth of spinal ganglia in plasma from vitamin B1-deficient chickens. *J Cell Comp Physiol* 1943;22:205–22.
- [22] Weiss P. The technology of nerve regeneration: a review. Sutureless tubulation and related methods of nerve repair. *J Neurosurg* 1944;1:400–50.
- [23] Merle M, Dellon AL, Campbell JN, Chang PS. Complications from silicon-polymer intubulation of nerves. *Microsurgery* 1989;10(2):130–3.
- [24] Evans GR, Brandt K, Widmer MS, Lu L, Meszlenyi RK, Gupta PK, et al. In vivo evaluation of poly(L-lactic acid) porous conduits for peripheral nerve regeneration. *Biomaterials* 1999;20(12):1109–15.
- [25] Silver FH, Christiansen DL. *Biomaterials science and biocompatibility*. New York: Springer-Verlag New York Inc; 1999.
- [26] Jeyanthi R, Rao P. In vivo biocompatibility of collagen-poly(hydroxyethyl methacrylate) hydrogels. *Biomaterials* 1990;11:238–43.
- [27] Smetana Jr. K, Sulc J, Krcova Z, Pitrova S. Intraocular biocompatibility of hydroxyethyl methacrylate and methacrylic acid copolymer/partially hydrolyzed poly(2-hydroxyethyl methacrylate). *J Biomed Mater Res* 1987;21(10):1247–53.
- [28] Navab M, Fogelman AM, Berliner JA, Territo MC, Demer LL, Frank JS, et al. Pathogenesis of atherosclerosis. *Am J Cardiol* 1995;76(9):18C–23C.
- [29] Berliner JA, Navab M, Fogelman AM, Frank JS, Demer LL, Edwards PA, et al. Atherosclerosis: basic mechanisms. Oxidation, inflammation, and genetics. *Circulation* 1995;91(9):2488–96.
- [30] Shanahan CM, Cary NR, Metcalfe JC, Weissberg PL. High expression of genes for calcification-regulating proteins in human atherosclerotic plaques. *J Clin Invest* 1994;93(6):2393–402.
- [31] Ikeda T, Shirasawa T, Esaki Y, Yoshiki S, Hirokawa K. Osteopontin mRNA is expressed by smooth muscle-derived foam cells in human atherosclerotic lesions of the aorta. *J Clin Invest* 1993;92(6):2814–20.
- [32] Thubrikar MJ, Deck JD, Aouad J, Nolan SP. Role of mechanical stress in calcification of aortic bioprosthetic valves. *J Thorac Cardiovasc Surg* 1983;86(1):115–25.
- [33] Whalen RL, Snow JL, Harasaki H, Nose Y. Mechanical strain and calcification in blood pumps. *Trans Am Soc Artif Intern Organs* 1980;26:487–92.